

# Designing $ABO_3$ structure with Lennard-Jones interatomic potentials

Hui Zhang,<sup>a)</sup> Zhongwu Liu, Xichun Zhong, Dongling Jiao, and Wanqi Qiu

*School of Materials Science and Engineering, South China University of Technology, Guangzhou 510640, People's Republic of China*

(Dated: 9 November 2021)

In this paper, our goal is to design  $ABO_3$  crystal structure with simple interatomic Lennard-Jones (LJ) potentials and without setting any initial Bravais lattice and it is carried out by molecular dynamics (MD) simulation. In the simulation, the equilibrium distances between atoms are determined by LJ potentials. For the identification of the microstructure of simulated system, we have calculated the distribution functions of both the angles between one atom and its nearest neighbors and the distances between atoms and compared the results with those of ideal lattices. The results have clearly shown that we have successfully produced  $ABO_3$  crystal structure by MD simulation.

## I. INTRODUCTION

Designing specific materials as needed is the goal of material scientists. However, this job is very difficult and more work is needed. In our previous work, it has been found that the interatomic potentials are very important for the formation of crystalline solids<sup>1,2</sup>. Very complex crystal structures such as diamond and graphite structures can be formed with simple LJ interatomic potentials. This means that it is possible for us to design the system with desirable crystal structure even though we have not learnt a lot about the interaction between atoms. In the simulation of the crystal structures reported in Refs. 1 and 2, both the interactions and the equilibrium distances between atoms are defined by LJ potentials. One question of whether we can design the crystal structures of material by using the equilibrium distances determined by LJ potentials arises. To answer this question, we can choose one well-known and complex structure as a target, design the crystal structure in terms of its lattice constants, and reproduce it by MD simulation.  $ABO_3$  structure, also called perovskite structure, is a very important crystal structure for many materials showing different functions such as ferroelectric crystals of  $BaTiO_3$  and  $PbTiO_3$ <sup>3</sup>, and perovskite solar cells<sup>4,5</sup>. In  $ABO_3$  structure, A atoms occupy the vortices of the cubic, B atoms the body center positions, and O atoms six face centers. We have taken  $AB_3$  structure as our target. In our strategy, the equilibrium distances between atoms are determined by the LJ potentials. If the lattice constant of  $ABO_3$  structure is  $a$ , then  $r_{AA}=a$ ,  $r_{BB} = a$ ,  $r_{OO} = 0.707a$ ,  $r_{AB} = 0.866a$ ,  $r_{AO} = 0.707a$ , and  $r_{BO} = 0.5a$ . With the above potential parameters, it is expected that the liquid-crystalline phase transition of  $ABO_3$  system can be reproduced by MD simulation and at crystalline state our simulated system shows a perfect  $ABO_3$  crystal structure. We identify the crystal structure of simulated system by calculating the distribution functions of both the angles between one atom and its nearest neighbors

and the distances between atoms for A-A, B-B, O-O, A-O, B-O, and A-B subsystems and checking the atomic arrangements.

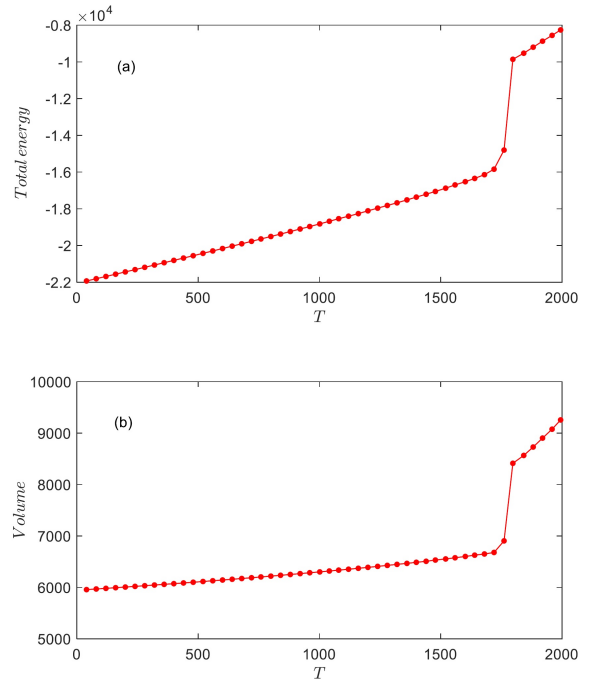


FIG. 1. Dependence of both the total energy (a) and volume (b) of simulated systems on the temperature.

## II. SIMULATION AND METHOD

We introduce the classic LJ potential to describe the interatomic coupling, and LJ potential can be written as

$$U(r) = 4\epsilon \left( \left( \frac{\sigma}{r} \right)^{12} - \left( \frac{\sigma}{r} \right)^6 \right) \quad (1)$$

where  $\epsilon$  is the depth of the potential well,  $\sigma$  is the finite distance at which the inter-particle potential is zero,

<sup>a)</sup>Electronic mail:zhope@scut.edu.cn

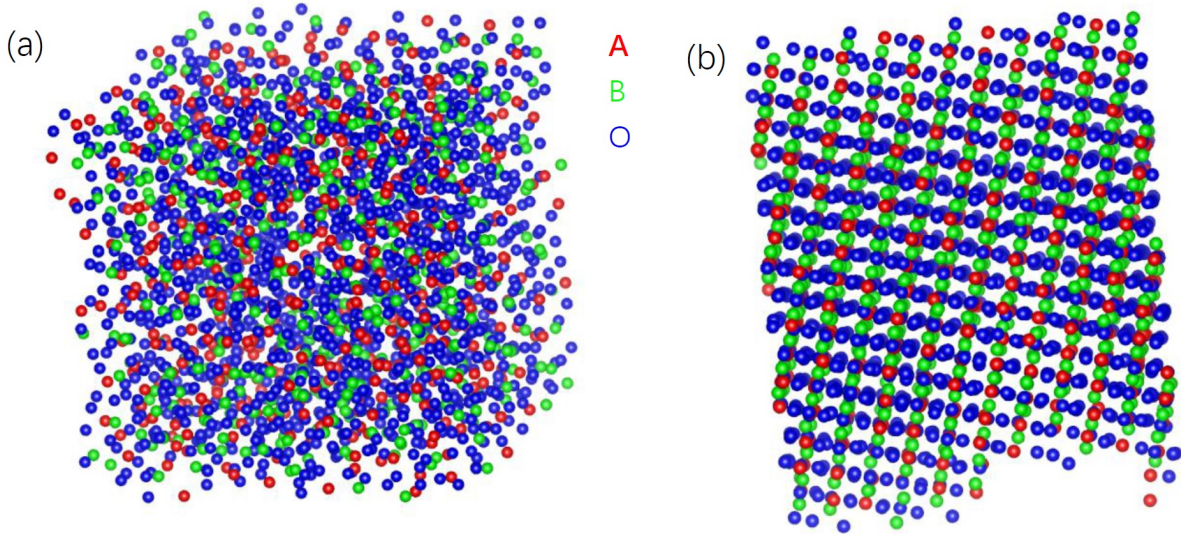


FIG. 2. The atomic arrangements of simulated system at the liquid state (a) and at the crystalline state (b).

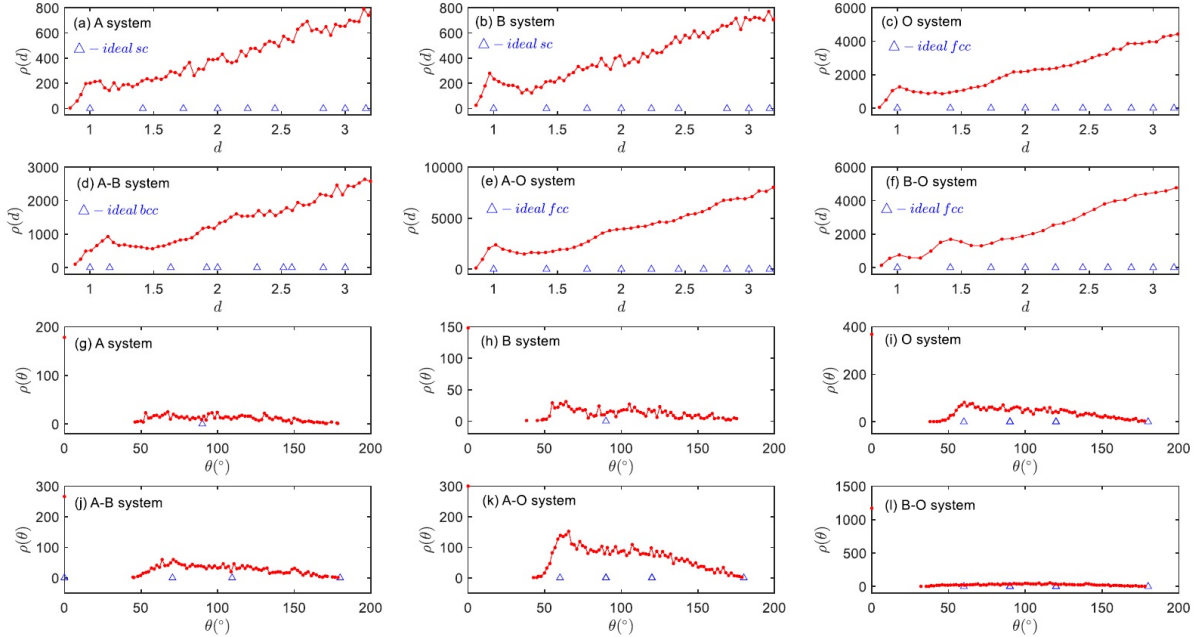


FIG. 3. At the liquid state, the distribution functions of both the angles between one atom and its nearest neighbors (a) and the distances between the atoms (b).  $\Delta$  denote the distribution functions for ideal lattices.

and  $r$  is the distance between particles. The distance of cutoff is denoted by  $r_c$ . The simulation was carried out with the aid of LAMMPS<sup>6</sup>. In the simulation, the LJ units were used, and the periodic boundary conditions were applied. We set  $r_c=3\sigma$ .  $\sigma_{AA}=2.0$ , and  $r_c=6.0$ .  $\sigma_{BB}=2.0$ , and  $r_c=6.0$ .  $\sigma_{OO}=1.414$ , and  $r_c=4.242$ .  $\sigma_{AB}=1.732$ , and  $r_c=5.196$ .  $\sigma_{AO}=1.414$ , and  $r_c=4.242$ .  $\sigma_{BO}=1.0$ , and  $r_c=3.0$ . The masses of the particles were all 100, and the numbers of particles were denoted by  $n$ .  $n_A=500$ ,  $n_B=500$ , and  $n_O=1500$ . We

did not set any initial Bravais lattice. The particles were created randomly in the simulation box and then an energy minimization procedure followed. The initial temperature  $T_0=\epsilon$ , and  $\epsilon=2000$ . We set the timestep as 0.001. At  $T_0$ , NPT dynamics was implemented for  $1 \times 10^6$  timesteps, and then the temperature was decreased by  $T_0/40$ . At every following temperatures  $T$ , NPT was carried out for a time of  $t$  timesteps, and  $t=10^6$ . The pressure was always zero in the simulation. Details can be found in in-script in Appendix. The visualization of

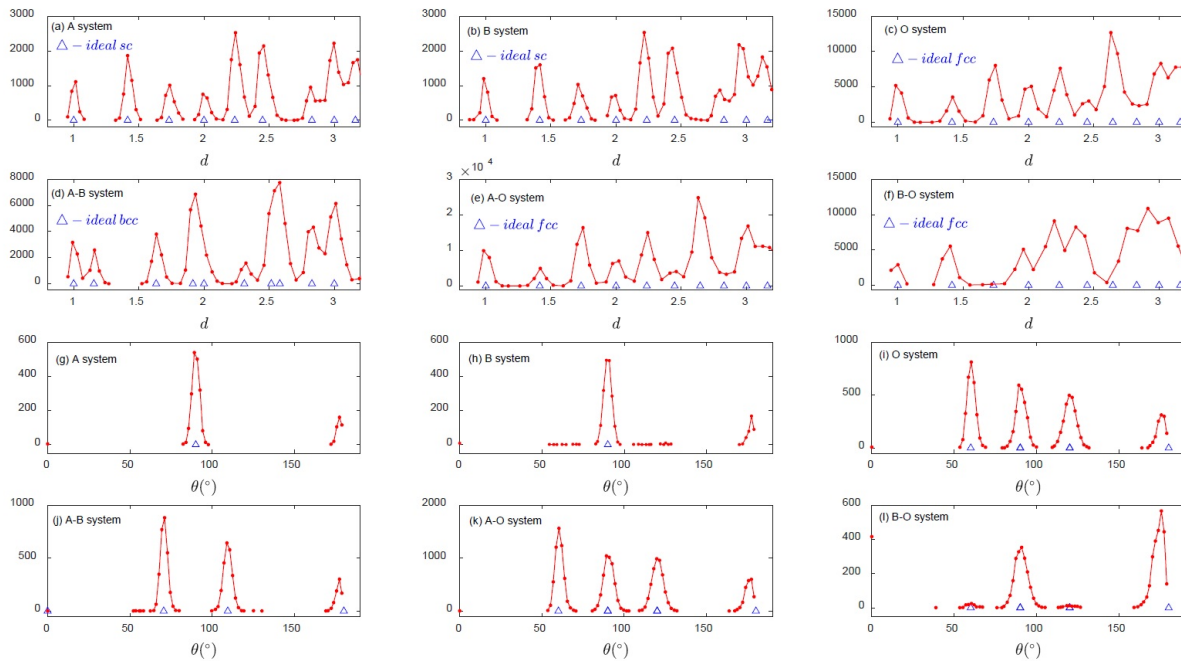


FIG. 4. At the crystalline state, the distribution functions of both the angles between one atom and its nearest neighbors (a) and the distances between the atoms (b).  $\Delta$  denote the distribution functions for ideal lattices.

simulated results was done with the aid of VESTA<sup>7</sup>. For LJ potential, the equilibrium distance  $r_0=1.12\sigma$ .

We calculated the distribution functions of both the angles between one atom and its nearest neighbors and the distances between atoms for the identification of microstructure of simulated system<sup>2</sup>. For more information, a set of A (or B and O) atoms was treated as a subsystem, and called A, B, and O systems. A-B system was set as a union of both A subsystem and B subsystem, and we had A-B, A-O, and B-O systems.

### III. RESULTS AND DISCUSSIONS

When  $ABO_3$  system is cooled from high temperature, there is a liquid-solid phase transition, and an abnormal jump in its volume. Figure 1 shows the dependence of both the total energy and volume of simulated system on the temperature. As shown in Fig. 1, sudden changes in the total energy and volume clearly show that there is a phase transition. This means that there is a disorder-order phase transition and an unusual change in the atomic arrangement. Figure 2 shows the atomic arrangements at the liquid and crystalline states. As shown in Fig. 2, the difference in the atomic arrangements is clear but we cannot determine which lattice the system shows. In order to identify the crystal structure, we calculated the distribution functions of both the angles between one atom and its nearest neighbors and the distances between atoms for A, B, O, A-B, A-O, and B-O

systems. When their distribution functions are in agreement with those of ideal lattices, we can make the final identification of the crystal structure. Figure 3 shows the distribution functions of both the angles between one atom and its nearest neighbors and the distances between atoms. As shown in Fig. 3, there are no clear peaks associate with a specific lattice, and our simulated system is in a liquid state. Figure 4 shows the distribution functions at crystallization state. In Fig. 4(a), A atoms form a simple cubic (sc) lattice, and the angles between its nearest neighbors are  $90^\circ$ . The ratios of the distances between atoms  $d_1: d_2: d_3: \dots=1: 1.414: 1.732: \dots$ , and the results are in agreement with data of ideal sc lattice, indicating that the atomic arrangements of A atoms are correct. In Fig. 4(b), B atoms occupy the body center of  $ABO_3$  structure, and all B atoms also form a sc lattice. In Fig. 4(c), O atoms occupy the face centers of  $ABO_3$  cubic, the angles between these O atoms are  $60^\circ$ ,  $90^\circ$ , and  $120^\circ$ . In Fig. 4(d), A and B atoms in  $ABO_3$  structure form a body-centered cubic (bcc) lattice, and the angles between A and B atoms and its nearest neighbors are  $70.5^\circ$  and  $109.5^\circ$ . In Fig. 4(e), A and O atoms form a face-centered cubic (fcc) lattice, and the angles between its nearest neighbors are  $60^\circ$ ,  $90^\circ$ , and  $120^\circ$ . In Fig. 4(f), B and O atoms form a tetrahedron, and the angles between B and O atoms are  $90^\circ$ . It has been shown from Fig. 4 that the calculated results are in agreement with those of ideal lattices and the atomic arrangement of A, B, and O atoms are correct. Therefore, we can initially identify the system showing  $ABO_3$  structure, and we further check the atomic arrangement for the final

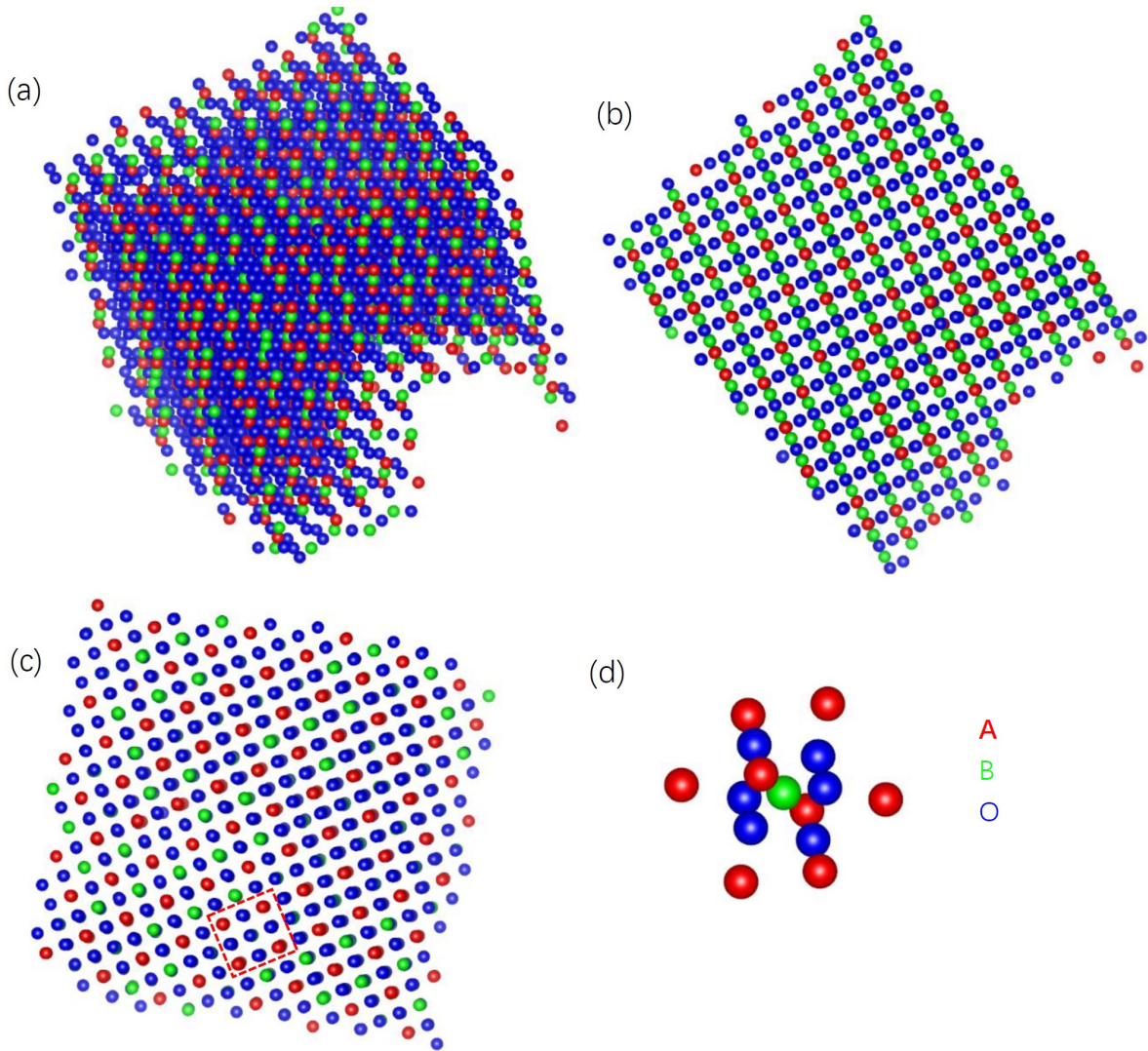


FIG. 5. (a)-(c) the atomic arrangements of simulated system observed from different directions, (d)  $ABO_3$  crystal cell obtained from the region encircled by the red dashed lines shown in (c).

identification.

Figure 5 shows the atomic arrangements of simulated system observed from different directions. As shown in Figs. 5(a)-(c), our simulated system is ordered, but we cannot make the final identification from these patterns. In Fig. 5(c), we tried to retrieve one  $ABO_3$  crystal cell. We removed the atoms outside the region encircled by the red dash lines and rotated the residual structure. The same operation was repeated, and we obtained the  $ABO_3$  crystal cell shown in Fig. 5(d). Till now, we finally identify the system showing the  $ABO_3$  structure.

It must be pointed out that we introduced in only the equilibrium distances between atoms and both the electric charge and electric spin are not involved.

#### IV. CONCLUSIONS

Without setting any initial Bravais lattice and with simple Lennard-Jones interatomic potentials, simulated system showing  $ABO_3$  structure has been produced by MD simulation. LJ potentials presented can not only describe the liquid-crystalline phase transition but also determine the crystal structure of simulated system.

#### Appendix A: in script

```

units          lj
boundary       p p p
atom_style     atomic
dimension      3
region         box block 0 20 0 20 0 20

```

```

create_box      3 box
create_atoms    1 random 500 245 box
create_atoms    2 random 500 255 box
create_atoms    3 random 1500 265 box
timestep        0.001
thermo          1000
group           big1 type 1
group           big2 type 2
group           big3 type 3
mass            1 100
mass            2 100
mass            3 100
variable        lcut1 equal 3.0
variable        lcut2 equal 4.242
variable        lcut3 equal 5.196
variable        lcut4 equal 6.0
variable        la equal 2000
pair_style      lj/cut ${lcut1}
pair_coeff       1 1 ${la} 2.0 ${lcut4}
pair_coeff       2 2 ${la} 2.0 ${lcut4}
pair_coeff       3 3 ${la} 1.414 ${lcut2}
pair_coeff       1 2 ${la} 1.732 ${lcut3}
pair_coeff       1 3 ${la} 1.414 ${lcut2}
pair_coeff       2 3 ${la} 1.0 ${lcut1}

minimize        1.0e-10 1.0e-10 1000000 &
1000000
dump            1 all image 1000 image.* &
.jpg type type zoom 1.6
run             1000
undump          1
variable        ltemp equal 1600
velocity        all create ${ltemp} &
314029 loop geom
fix             1 all npt temp ${ltemp} &
${ltemp} 1.0 iso 0.0 &
0.0 1.0
dump            1 all image 500000 image &
.*.jpg type type zoom 1.6
dump            2 all xyz 500000 file1.&

```

```

*.xyz
run             1000000
undump          1
undump          2
variable        lpa equal ${ltemp}
label           loopa
variable        a loop 39
variable        tem equal ${lpa}-40*$a
fix             1 all npt temp ${tem} &
${tem} 1.0 iso 0.0 0.0 1.0
dump            1 all image 5000 image.* &
.jpg type type zoom 1.6
dump            2 all xyz 5000 file1.*.xyz
run             1000000
undump          1
undump          2
next            a
jump            SELF loopa

```

## ACKNOWLEDGMENTS

This work is supported by the National Natural Science Foundation of China (Grant No. 11204087).

<sup>1</sup>H. Zhang, Z. Liu, X. Zhong, D. Jiao, W. Qiu, Molecular dynamics simulation of crystallization and non-crystallization of Lennard-Jones particles without setting any initial Bravais lattice, arXiv:1805.07767.

<sup>2</sup>H. Zhang, Z. Liu, X. Zhong, D. Jiao, W. Qiu, Molecular dynamics simulation of diamond and graphite structures without setting any initial Bravais lattice and with Lennard-Jones interatomic potentials, arXiv:1805.10614.

<sup>3</sup>K. M Rabe, J.-M. Triscone, C. H Ahn. Physics of ferroelectrics: a modern perspective (Springer, Heidelberg, 2007).

<sup>4</sup>B. V. Lotsch, New light on an old story: perovskites go solar, Angew. Chem. Int. Ed. 53, 635 (2014).

<sup>5</sup>D. B. Mitzi, C. A. Field, W. T. A. Harrison, A. M. Guloy, Nature, 369, 467 (1994).

<sup>6</sup>S. J. Plimpton, Fast parallel algorithms for short-range molecular dynamics, J. Comp. Phys., 117, 1 (1995).

<sup>7</sup>K. Momma, F. Izumi, VESTA 3 for three-dimensional visualization of crystal, volumetric and morphology data, J. Appl. Crystallogr., 44, 1272 (2011).